Experimental and Molecular Pathology 104 (2018) 190–198

Contents lists available at ScienceDirect

Experimental and Molecular Pathology

journal homepage: www.elsevier.com/locate/yexmp

CD10 inhibits cell motility but expression is associated with advanced stage disease in colorectal cancer

Teresa P. Raposo[a,b,*], Mireia Sueca Comes[c], Adeyemi Idowu[a], Bora Agit[a], James Hassall[a,b], Wakkas Fadhil[a,b], Robert Nica[d], Rupert Ecker[d], Takashi Yao[e], Mohammad Ilyas[a,b]

[a] Division of Cancer and Stem Cells, School of Medicine, University of Nottingham, United Kingdom
[b] Nottingham Molecular Pathology Node, United Kingdom
[c] Biochemistry and Molecular Biology, University Rovira i Virgili, Tarragona, Spain
[d] Tissue Gnostics GmbH, Vienna, Austria
[e] Department of Human Pathology, Juntendo University, School of Medicine, Tokyo, Japan

ARTICLE INFO

Keywords:
CD10
NEP
CALLA
Colorectal cancer
Epithelial-mesenchymal transition
Metastasis

ABSTRACT

Introduction: CD10 is a cell membrane-bound endopeptidase which is expressed in normal small bowel but not in normal colon. It is aberrantly expressed in a small proportion of colorectal cancers (CRC) and this has been associated with liver metastasis and poor prognosis. We sought to investigate the mechanism of CD10 activity and its association with clinicopathological features.

Material and methods: CD10 was stably knocked down by lentiviral shRNA transduction in the CRC cell lines SW480 and SW620 which are derived from a primary tumour and its corresponding metastasis respectively. Expression of epithelial – mesenchymal transition (EMT) markers was tested as well as the effect of knockdown on cell viability, migration and invasion assays. In addition, immunohistochemical expression of CD10 in primary colorectal tumours (N = 84) in a tissue microarray was digitally quantified and analysed for associations with clinicopathological variables.

Results: Knockdown of CD10 did not alter cell viability in SW480, but migration and invasion levels increased ($P < 0.001$ for each) and this was associated with a cadherin switch. In SW620, CD10 knockdown caused a reduction in cell viability after 72 h ($P = 0.0018$) but it had no effect on cell migration and invasion. Expression of epithelial CD10 in primary tumours was associated with presence of lymph node invasion ($P = 0.001$) and advanced Duke's stage ($P = 0.001$).

Conclusions: Our results suggest that the function of CD10 may change during tumour evolution. It may inhibit cell motility in early-stage disease whilst promoting cell viability in late-stage disease. It has a complex role and further studies are needed to elucidate the suitability of CD10 as a prognostic marker or therapeutic target.

1. Introduction

CD10 (cluster of differentiation 10, also designated as neprylisin, membrane metallo-endopeptidase (MME), neutral endopeptidase (NEP) and common acute lymphoblastic leukemia antigen (CALLA) is a zinc-dependent metalloendoprotease which degrades peptides involved in cancer signaling pathways (Maguer-Satta et al., 2011). CD10 is expressed in a variety of cells. It is expressed in bone marrow lymphoid stem cells, pro-B lymphoblasts, and mature neutrophils and it is used for classification of leukaemias and malignant lymphomas (Lu et al., 2016). It is also seen in the endometrial stroma and, with regards to the epithelium, it is found to be expressed in the lumina of renal tubules, hepatic sinusoids and the microvilli of the small intestine (Iwase et al., 2014; Katano et al., 2017; Lloyd and Owens, 2011).

In solid tumours, CD10 over-expression has found use as a diagnostic marker to distinguish benign from malignant breast phyllodes tumours (Ibrahim, 2011; Puri et al., 2016; Tariq et al., 2015) and it has been associated with a poor prognosis in malignant breast cancer (Jana et al., 2014). Similarly, in prostatic cancer cases, CD10 expression was found to correlate with elevated pre-operative prostate-specific antigen (PSA), higher Gleason score and advanced stage (Fleischmann et al., 2008).

CD10 is normally absent in healthy colonic mucosa but it can be aberrantly expressed in both the epithelium and stroma of colorectal

* Corresponding author at: West block, D floor, Cancer Biology Unit, Division of Cancer and Stem Cells, Queen's Medical Centre, University of Nottingham, Derby Road, Nottingham NG7 2UH, United Kingdom.
E-mail address: msztp2@nottingham.ac.uk (T.P. Raposo).

https://doi.org/10.1016/j.yexmp.2018.04.002
Received 13 December 2017; Accepted 9 April 2018
Available online 11 April 2018
0014-4800/ © 2018 Elsevier Inc. All rights reserved.

tumours and an association with advanced disease is reported (Ogawa et al., 2002). It is not expressed in adenomas with low grade dysplasia but aberrant expression – in both stromal and epithelial compartments – is seen in adenomas with high-grade dysplasia and in invasive adenocarcinomas (Ogawa et al., 2002). CD10 expression has also been associated with increased tumour invasiveness, accumulation of p53 and large tumour size (Ogawa et al., 2002). Moreover, CD10 expression is a significant risk factor for the development of liver metastasis (Fujita et al., 2010; Ohji et al., 2007) and elevated CD10 serum levels have also been shown to be specific predictors of synchronous and metachronous liver metastasis in a cohort of human patients (Sasaki et al., 2014). In a mouse model of metastatic colorectal cancer, CD10 causes degradation of the anti-proliferative protein hepatic met-enkephalin thereby enhancing tumour growth (Kuniyasu et al., 2010).

CD10 may also play a role in metastasis in CRC. For metastasis, cells need to undergo epithelial to mesenchymal transition (EMT). During EMT epithelial cells lose their junctions, reorganise their cytoskeleton and undergo a transformational morphological and programming change, which consequently enables an invasive phenotype (Lamouille et al., 2014). Invasive cells may reach blood vessels, circulate to distant organs and settle at the secondary site. For growth at the metastatic site, cells need to undergo the reverse process of mesenchymal to epithelial transition (MET) resulting in formation of metastatic deposits.

We hypothesized that CD10 may have a role in the formation of metastasis through the regulation of the EMT and/or MET processes and thereby altering the motility and invasion of colorectal cancer cells. To test this hypothesis, a stable CD10 knockdown was performed by lentiviral transduction of shRNA in two cell lines obtained from the same patient but derived from the primary tumour and its corresponding metastasis. This allowed us to perform functional assays to assess the role of CD10 at the different stages of colorectal cancer in cells with the same genetic background.

2. Material and methods

2.1. Cell culture

Colorectal Cancer cell lines SW620 (ATCC® CCL-227™) and SW480 (ATCC® CCL-228™) were grown in complete high-glucose DMEM (Dulbecco's Modified Essential Medium; Gibco® Life Technologies) supplemented with 2 mM L-glutamine and 10% fetal bovine serum (Sigma Aldrich) and incubated at 37 °C, 5% CO_2 atmosphere in a humidified incubator.

2.2. Lentiviral transduction of shRNA targeting CD10 and luciferase

The short hairpin RNA (shRNA) for CD10 and LUC (Luciferase) knockdown were selected using the online tool 'siRNA at Whitehead' (freely available from http://sirna.wi.mit.edu/home.php), using the pattern N2[CG]N8[AUT]N8[AUT]N2 and filtering off-targets with least three mismatches (Pei and Tuschl, 2006).

The shRNA oligos (Table 1) were annealed at 95 °C for 4 min in a PCR thermal cycler and slowly cooled down overnight. The annealed oligos were ligated into pLKO.1-TRC (Addgene plasmid #10878), transformed in chemocompetent *E.coli*, isolated by miniprep and double-digested with restriction enzymes *Age*I and *Eco*RI. Correctly inserted oligos were confirmed by restriction enzyme double-digestion with EcoRI and *Nco*I of the resulting vectors and sequencing. Restriction enzymes and chemocompetent *E. coli* were supplied by New England Biolabs.

Viral particles were packaged in HEK293T cells seeded at a density of 1.5×10^6/10 cm petri dishes in a proportion of 24 µL Fugene 6 (Promega, E2691) in 136 µL serum-reduced OPTI-MEM (Gibco, Invitrogen) to 2 µg pLKO.1 shRNA plasmid: 1500 ng psPAX2 packaging plasmid (Addgene #12260): 500 ng pMD2.G envelope plasmid (Addgene #12259) to 40 µL serum-reduced OPTI-MEM. After transfection, shRNA lentiviruses were concentrated by ultracentrifugation at 10,000 × *g*, 4 °C, 4 h in a 10% sucrose buffer (Jiang et al., 2015).

For stable transfection, SW480 and SW620 cells were pre-treated with 8 µg/mL polybrene (Sigma-Aldrich, #H9268) for 10 min and transduced with viral particles containing transfer vectors pLKO.1-TRC-shCD10 or pLKO.1-TRC- shLUC (negative control) for at least 48 h. Transduced cells were selected by treatment with puromycin (Sigma-Aldrich, #P8833) at a pre-tested concentration between 5 and 10 µg/mL which caused 100% cell death in untransduced cells. Lentiviral particle production and transduction procedures were adapted from the available protocol supplied by Addgene (Plasmid 10,878. Protocol Version 1.0. December 2006), previously used in the preparation of lentiviral shRNA libraries (Moffat et al., 2006). CD10 knockdown in SW620 is annotated as $SW620^{CD10-}$, whilst luciferase controls are annotated as $SW620^{LUC-}$. A similar annotation scheme is used for SW480.

2.3. Protein extraction and Western blot

Cells were washed with ice-cold PBS and incubated on ice for 10 min with RIPA buffer with protease and phosphatase inhibitor diluted to 1 ×. The resulting cell lysates were centrifuged at 16000*g*, at 4 °C for 30 min and the supernatant transferred to a new eppendorf tube. Protein quantification of the supernatant was performed with the Pierce® BCA Assay Kit (Thermo Scientific) according to manufacturer's instructions.

For Western blotting, 50 µg of protein sample mixed with 25% (v/v) NuPAGE® LDS Sample buffer(4 ×) and 10%(v/v)reducing sample buffer (10 ×) were denatured at 95 °C for 5 min, incubated in ice for 5 min and then loaded into to a pre-cast gel (NuPAGE® 4–12% Bis-Tris Protein Gels, Invitrogen). Gel electrophoresis was performed for 90 min at 125 V. The resulting gel was immunoblotted onto a polyvinylidene difluoride (PVDF) membrane (Amersham, GE Healthcare Life Sciences) at 25 V for 30 min, using the BIO-RAD® Trans-Blot Transfer system.

After confirming transfer by Ponceau Red staining, blocking to prevent non-specific protein binding was carried out by incubating the membrane with 5% skimmed milk (Sigma-Aldrich) or bovine serum albumin (BSA) (ThermoFisher Scientific) in tris-buffered saline 0.1% Tween-20 (TBST) for 1 h with gentle agitation at room temperature. The membrane was incubated overnight with primary antibody, at 4 °C with gentle agitation and then was washed 3 × 5 min with TBST. It was incubated with the appropriate HRP-conjugated secondary antibody for 1 h at room temperature, using the blocking solution as the diluent. Diluents and antibodies used are detailed on Table A1 (Supplementary data). The membrane was further washed 3 × 5 min in TBST and chemiluminescence was developed using the Amersham ECL Western Blotting Detection Reagent (GE Healthcare Life Sciences). Immunoblots

Table 1
shRNA oligonucleotides for CD10 and LUC.

shRNA oligo (5′-3′)	
CD10 sense	CCGGGCTGGTTGAAACGTAATGTTTCTCGAGTTCGACCAACTTTGCATTACATTTTTG
CD10 antisense	AATTCAAAAAGCTGGTTGAAACGTAATGTTTCTCGAGTTCGACCAACTTTGCATTACA
LUC sense	CCGGGGCGGAAAGTCCAAATTGTTTCTCGAGTTCCGCCTTTCAGGTTTAACATTTTTG
LUC antisense	AATTCAAAAAGGCGGAAAGTCCAAATTGTTTCTCGAGTTCCGCCTTTCAGGTTTAACA

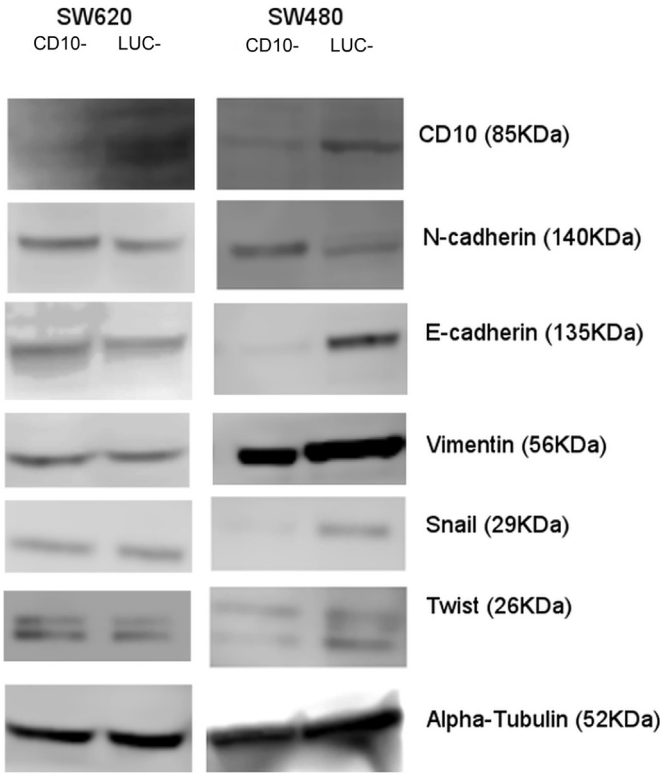

Fig. 1. Confirmation of CD10 knockdown by western blot and alterations of EMT markers, validated in two independent experiments.

were scanned and analysed by densitometry with the C-DiGit® Blot scanner and Image studio system (LI-COR). Ratios of Target protein/ α-Tubulin intensity ratio and the relative knockdown (KD *vs* Luciferase control) were calculated (Supplementary Fig. A1).

2.4. Immunofluorescence staining

$SW620^{CD10-}$, $SW620^{LUC-}$, $SW480^{CD10-}$ and $SW480^{LUC-}$ were seeded at a density of 2.0×10^4 cells per well of a chamber slide and incubated overnight at 37 °C in a 5%CO_2 incubator. Cells were washed in PBS (phosphate buffered saline), fixed by incubation in 4% paraformaldehyde, permeabilized by 0.1% triton-× 100 PBS and blocked for 1 h with 1%BSA, 0.1% tween 20, 22.52 mg/mL glycine PBS. CD10 rabbit anti-human antibody diluted 1:100 (Abcam, EPR5904-110 ab208778) and alpha-tubulin mouse anti-human diluted 1:200 (Abcam, DM1A ab7291), were incubated overnight at 4 °C, after 3 × 5 min washes in 0.1%Tween 20 in PBS (PBST) secondary antibodies Alexa-Fluor 568 goat anti-rabbit secondary antibody and Alexa-Fluor 488 goat anti-mouse secondary antibody (Invitrogen) were incubated for 1 h, followed by another 3 × 5 min washes in PBST. Nuclei were stained by incubation with DAPI (Sigma Aldrich) diluted 1:5000, for 15 min and slides were mounted with fluoroshield anti-fade mountant (Sigma Aldrich). The slides were imaged on a Leica SP2 confocal microscope using the 63× objective with immersion oil.

2.5. Cell viability assays and cell cycle analysis

For cell viability, 1×10^4 cells of each condition of interest (*i.e.* $SW620^{CD10-}$, $SW620^{LUC-}$, $SW480^{CD10-}$ and $SW480^{LUC-}$) were seeded in each well of a 96 well plate. For each condition, 12 replicate wells were seeded and an individual plate was set up for each of 4 time points.

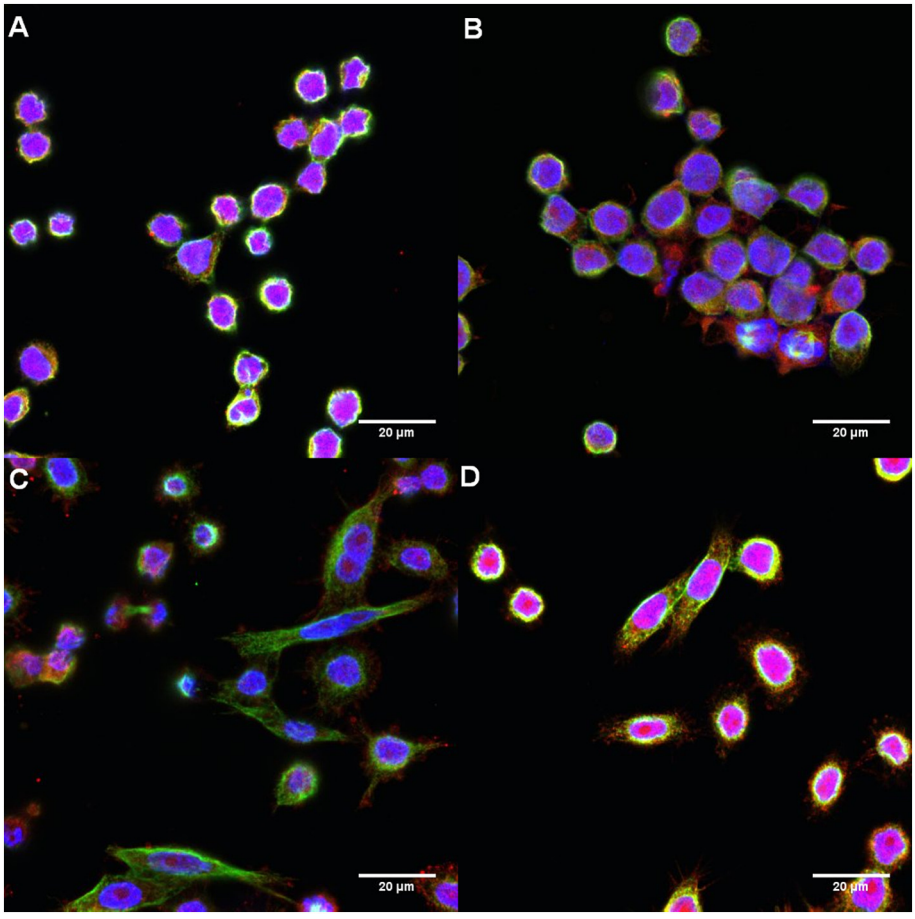

Fig. 2. Confocal imaging of immunofluorescence staining of CD10 labelled red with Alexa-Fluor 568 goat anti-rabbit secondary antibody in $SW620^{CD10-}$ (A), $SW620^{LUC-}$ (B), $SW480^{CD10-}$ (C) and $SW480^{LUC-}$ (D).Cytoplasmic staining by alpha-tubulin (1:200) labelled green with Alexa-Fluor 488 goat anti-mouse secondary antibody (Invitrogen). Nuclear staining by DAPI is shown in blue. (For interpretation of the references to colour in this figure legend, the reader is referred to the web version of this article.)

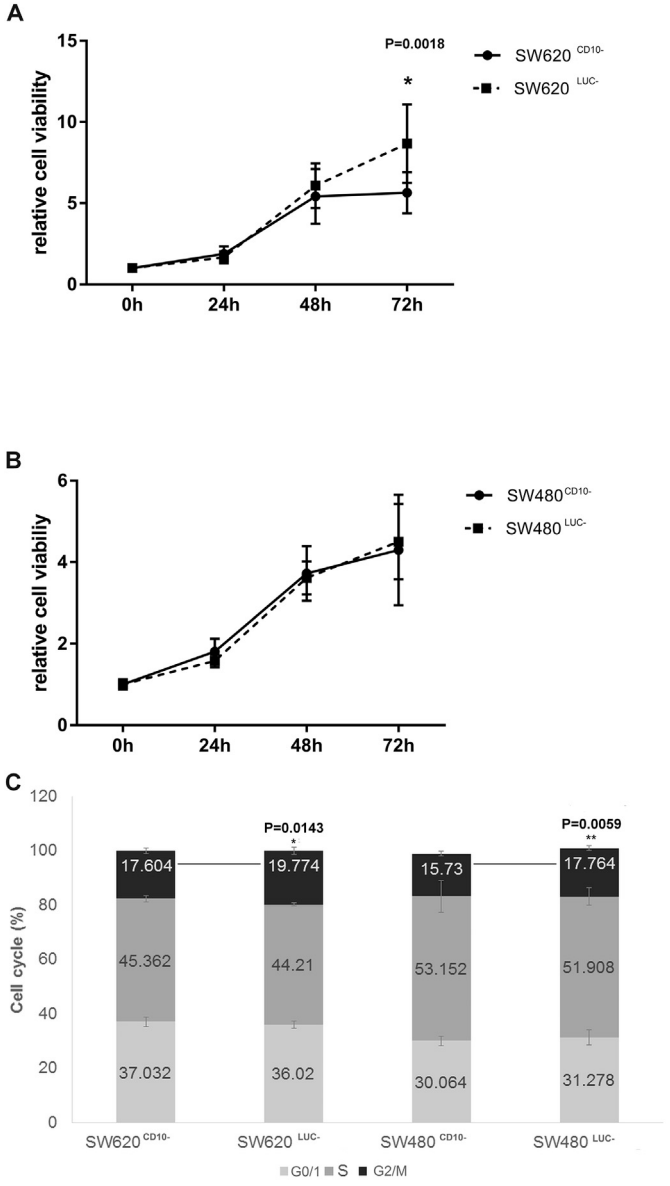

Fig. 3. Relative cell viability values, normalised to the first reading taken at 0 h showing no difference for SW620 (A and C) and SW480 (B and D) respectively. Cell cycle analysis shows a small decrease on G2/M phase of growth arrest in shCD10 transduced cells** = P < 0.01, * = P < 0.05.

Cells were cultured in a volume of 100 µL and incubated at 37 °C, 5% CO_2. Cell viability was quantified using a resazurin-based assay with PrestoBlue® Cell Viability Reagent (Invitrogen) diluted to 10% in cell culture media. To allow correction to the background fluorescence 6 control wells containing only the assay reagent were included. The plate was incubated at 37 °C for 1 h and relative fluorescence was read at 544 nm excitation and 612 nm emission (FlexStation 384, Molecular Devices). Readings were taken at 0, 24, 48 and 72 h. To compare between different cell lines, RFU values were normalised to the first performed reading and results expressed as relative cell viability.

For the cell cycle analysis, 1×10^5 cells of each transduced type were seeded into each well of a 24-well plate in quintuplicates and incubated overnight at 37 °C, 5% CO_2. A single cell suspension was obtained by trypsinization, washed in PBS and fixed in 70% cold ethanol for 30 min at 4 °C, washed twice in PBS and treated with 50 µL of a 100 µg/mL stock solution of RNAse (Qiagen). Cells were again re-suspended in 300 µL of PBS and nucleic acids stained with 10 µL of propidium iodide stock solution at 1 mg/mL (Sigma Aldrich).

Table 2
Associations between clinicopathological variables and the epitehlial and stromal CD10 expression ratios. Pearson Chi-square was used to compare the CD10 high or low total epithelial and stromal scores for each of the categories considered. P-values < 0.05 are considered statistically significant and are highlighted in bold.

	Epithelial CD10 score		P-value	Stromal CD10 score		P-value
	Low	**High**		**Low**	**High**	
Grade						
1	1	1	0.397	1	1	0.380
2	33	35		35	32	
3	4	1		1	4	
Tumour invasiveness[a]						
1 or 2	9	5	0.258	5	9	0.235
3 or 4	29	32		32	28	
Duke's stage						
A and B	30	7	**0.001**	24	24	0.871
C1 and C2	16	21		12	13	
Ressection margin						
Free	35	35	0.572	33	35	0.954
Involved	1	2		2	2	
Vascular invasion						
Present	15	22	0.083	18	16	0.641
Absent	23	15		19	21	
LN metastasis						
Present	17	20	**0.001**	26	11	0.619
Absent	31	7		11	13	
KRAS status						
Wild-type	21	13	0.745	14	26	**0.034**
Mutant	21	11		16	10	

[a] Tumour invasiveness categories grouping corresponds to: Submucosa invasion (1); Muscularis propria invasion (2); Muscularis and pericolorectal invasion (3); Visceral peritoneum and organs (4).

Acquisition was performed on the FL3 channel of a Cytomics FC500 (Beckman Coulter) and cell cycle parameters analysed on Weasel v 3.0.

2.6. Migration and invasion assays

Cell migration and invasion assays were performed using 24-well polycarbonate transwell membrane inserts (pore size 8 µm; Corning®). For the migration assay, 1×10^5 cells were added to the uncoated transwell membrane inserts in 100 µL. For the invasion assay, matrigel Matrix (Corning® Matrigel® Matrix) diluted in cold PBS (100 µL, 300 µg/mL) was incubated for 2 h at 37 °C to coat the transwell insert.

For both the migration and invasion assays, cells were seeded in the top chamber in serum-free DMEM. DMEM with 10% FBS, 2 mM L-Glutamine (650 µL) was used as a chemoattractant in the receiver well. Quintuplicates of the CD10 knockdown and luciferase control were used for both assays and for each condition wells were established without chemoattractant as a negative control for the motility inducing effects of the serum.

After 24 h incubation, non-invading cells were removed from the upper chamber. The bottom of the transwells was trypsinized (650 µL trypsin) and trypsinized cells were transferred to the previous receiver well and stained with 4 µM of live-cell stain calcein AM (ThermoFisher Scientific) by incubation for 30 min at 37 °C under 5% CO_2.

The receiver wells were imaged using an inverted fluorescent microscope at 10× magnification on the FITC channel. To calculate the total number of cells per insert, the mean total number of cells per random microscope field of view (0.055µm^2) was counted in 4 fields of view and used to estimate the total number of migrated cells present at the bottom of the well (1.9cm^2). Quintuplicates were compared for CD10 knockdown and luciferase control cells. Control wells included no chemoattractant and also no coating for the invasion assay.

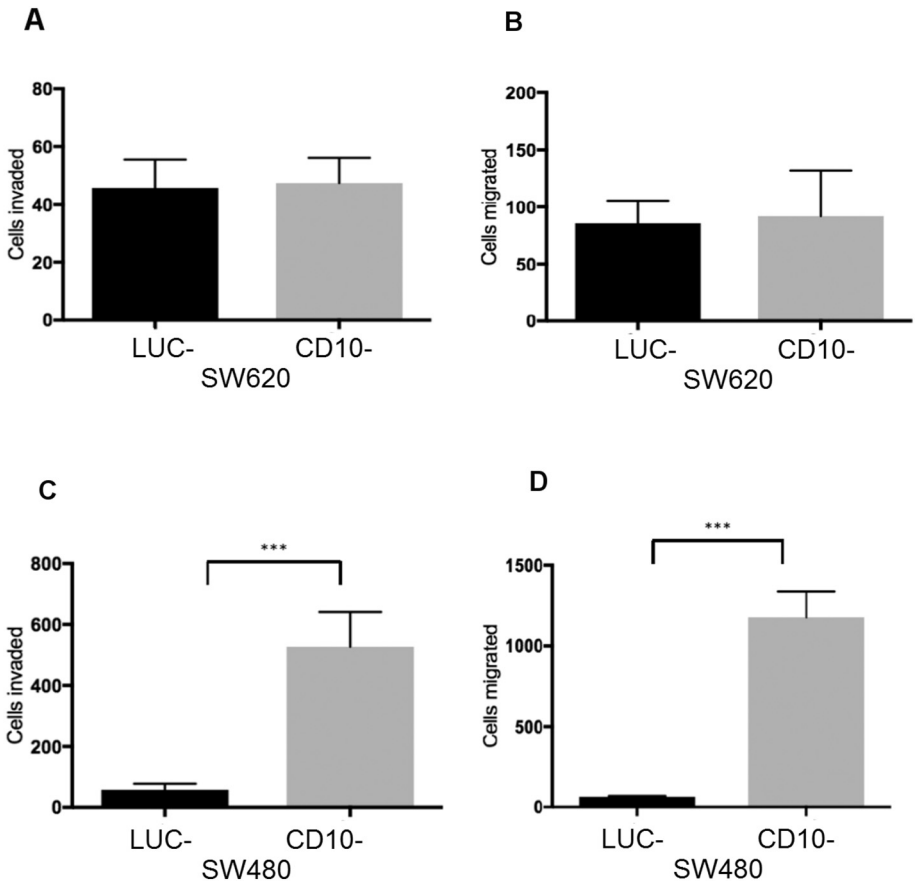

Fig. 4. Invasion and migration assays in $SW620^{CD10-}$ $SW620^{LUC-}$ (A and B) and $SW480^{CD10-}$ $SW480^{LUC-}$ (C and D). *** = $P < 0.001$ Mann-Whitney non-parametric *t*-test.

2.7. Immunohistochemistry (IHC) technique on tissue microarrays (TMAs)

Immunohistochemical (IHC) staining was performed on a tissue microarray slides (TMA) made from a series of 84 primary colorectal cancers. This series was created specifically for the purpose of evaluating biomarker expression in colorectal tumours and there was an unbiased selection of consecutive cases collected in Nottingham Sciences Biobank at the Queens Medical Centre, Nottingham, UK. Local ethical approval was granted prior to the construction of the TMAs, destined to IHC studies. Formalin-fixed paraffin embedded tissue blocks were retrieved from the archives and a TMA established as previously described (Albasri et al., 2014).

The TMA set included cores collected from luminal, mid-tumour, advancing edge areas of each tumour and, where possible, adjacent normal areas. Information on clinicopathological parameters tumour grade, primary tumour invasion, vascular invasion, Duke's stage, resection margin, KRAS mutation status and presence of lymph node metastasis was retrieved from histopathology reports preserving the patient anonymity. A summary of the clinicopathological characteristics in the tumour series studied is shown on table B1.

Tissue sections of 4 μm thickness were prepared onto poly-L-lysine coated slides (ThermoFisher Scientific, Menz glaser), deparaffinised in xylene, rehydrated by immersion in graded methanol and equilibrated in running tap water for 5 min.

Heat-induced antigen retrieval was performed by immersing the tissue sections in 1 mM EDTA buffer pH 9.0 microwaved for 20 min at 95 °C. After cooling, slides were mounted in Shandon coverplates and sequenza racks (ThermoFisher Scientific) for the remainder IHC incubation steps. For the rest of the procedure, underlined reagents are components of the Novolink Polymer kit (Leica Microsystems) and were used according to manufacturer's instructions. Endogenous peroxidases were blocked using peroxidase block for 5 min. Non-specific antibody binding was blocked by incubation with protein block for 5 min and washed in TBS (tris-buffered saline).

Each slide was incubated overnight at 4 °C with rabbit anti-Human CD10 primary antibody (cloneEPR5904-110, ab208778, Abcam) at a 1:2000 dilution. An isotype control anti-rabbit IgG was used at the same concentration as the primary antibody. After 3 × 5min washes with TBS, Post-primary reagent was incubated for 30 min at room temperature, followed by 3 × 5 min TBST washes and incubation with Novolink Polymer for 30 min. Diaminobenzidine (DAB) working solution was applied for 5 min, followed by a final wash in TBS.

Slides were then counterstained using haematoxylin and excessive stain removed by washes in tap water. After dehydration in methanol and xylene sections were mounted using mounting medium (DPX).Finally, slides were digitalised using a nanozoomer scanner (Hammamatsu).

Digital image analysis was performed on the software Strataquest v.6.0 (Tissue Gnostics). After colour separation and classifier-based tumour epithelium-stroma segmentation, ratios (%) were calculated for the CD10 positive epithelial area in the total tumour epithelium and CD10 positive stromal area within the total tumour stroma of each individual core. Misidentified epithelial and stromal areas were manually corrected if needed after individual verification of the segmentation results. The values of CD10 positive epithelium ratios for luminal, mid-tumour and advancing edge cores were added to calculate the total CD10 epithelium score.

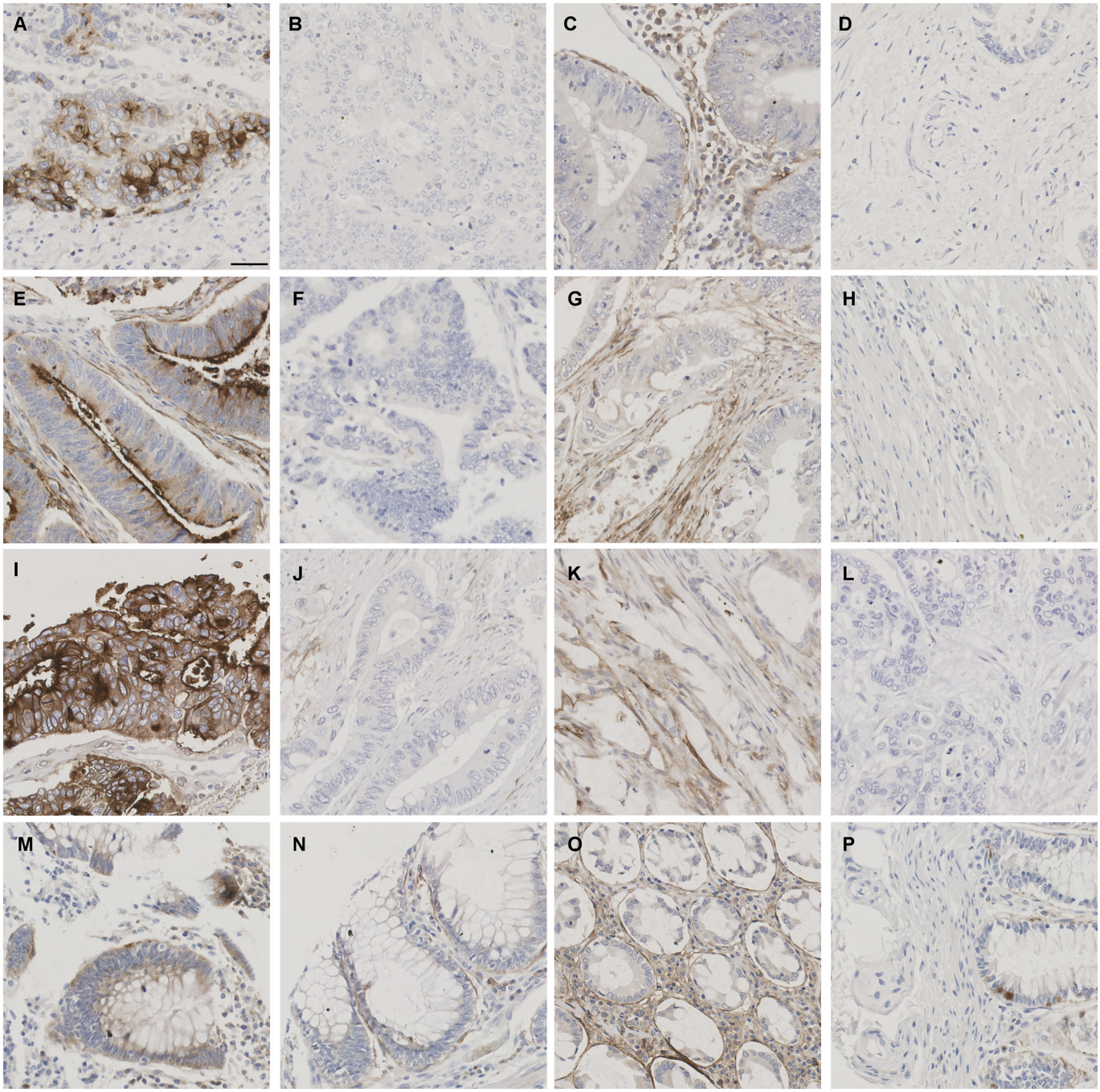

Fig. 5. Colorectal tumour luminal cores (A, B, C and D), mid-tumour cores (E, F, G, H), advancing edge cores (I, J, K, L) and adjacent normal (M, N, O and P). High (A, E, I, M) and low or negative (B, F, J, N) CD10 expression in the epithelial compartment. High (C, G, K, O) and low or negative (D,H,L,P) CD10 expression in the stromal compartment. All images were taken at the same magnification (200×), scale bar(A) = 40 μm.

2.8. Statistical analysis

GraphPad Prism 7.01 (CA, USA) was used for statistical analysis of *in vitro* assays. Two-way analysis of variance (ANOVA) was performed to analyse proliferation assays and cell cycle analysis. Unpaired Mann-Whitney *t*-test (non-parametric test) was performed to compare means in protein expression, migration and invasion assay results. The statistical software SPSS (Statistical Package for the Social Sciences, IBM, OH, USA) version 22.0 was used for IHC statistical analysis of associations with clinicopathological variables by Pearson Chi-square test. The normality test Kolmogorov–Smirnov was firstly applied to confirm the population followed a non-Gaussian distribution. Cut off values were determined by the median value of the total epithelial or stromal CD10 score. In all statistical comparisons, $p < 0.05$ was accepted as denoting significance difference.

3. Results

3.1. Confirmation of CD10 knockdown by western blot and immunofluorescence

After transduction with lentiviruses expressing shCD10 or shLUC oligos, the protein level was measured by Western Blot. CD10 protein expression was visibly decreased for both transduced shC10 cell lines

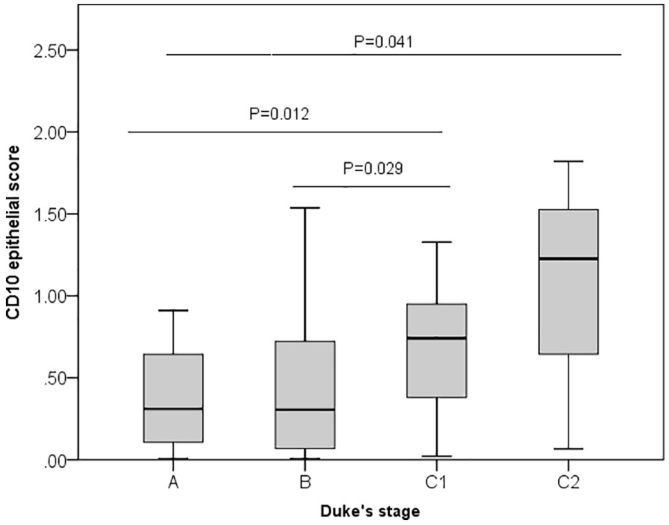

Fig. 6. Distribution of CD10 epithelial score across Duke's stage A,B,C1 and C2. There are statistically significant differences in CD10 epithelial score between Duke's stage A and C1 (P = 0.012), between B and C1 (P = 0.029) and A and C2 (*P* = 0.041) (Mann-whitney non parametric ranks comparison, exact, 2-sided).

(SW480^{CD10-} and SW620^{CD10-}, Fig. 1). These changes were also visible by immunofluorescence staining of CD10, where the fusiform morphology acquired by SW480^{CD10-} could also be observed (Fig. 2).

3.2. Effect of CD10 knockdown on cell viability

Cell viability was assessed at over a time course of 72 h. In SW480^{CD10-} cell viability was not altered as growth curves of the cells were identical to SW480^{Luc} (Fig. 3A). In contrast, in SW620^{CD10-} a delayed inhibition of cell growth which only became apparent after 72 h (Fig. 3B and B1). A cell cycle analysis confirmed a small but significant decrease in the G2/M phase post CD10 knockdown in SW620^{CD10-} and SW480^{CD10-} (P = 0.0143 and P = 0.0059 respectively, Fig. 2C).

3.3. Effect of CD10 knockdown on cell migration and invasion

Since no difference was observed in the effect of CD10 knockdown on the proliferative activity at 24 h, there was no need to block cell replication before performing migration and invasion assays (which are conducted in 24 h). In SW480^{CD10-} cells, the knockdown of CD10 resulted in an increase in cell motility. A statistically significant increase in cell numbers was observed in both the transwell migration and invasion assays when compared to the control cell line (P < 0.001) (Fig. 3C and D). In contrast, in SW620^{CD10-}, no significant differences were observed in either transwell migration or invasion assays between CD10 knockdown and luciferase control (Fig. 3A and B).

3.4. Identification of CD10-associated EMT markers

Expression of a variety of biomarkers related to the EMT process was assessed by Western blot. E-Cadherin and N-Cadherin are cell adhesion molecules and ordinarily, in the non-motile state, E-cadherin levels are high whilst N-Cadherin levels are low. When cells become motile, the levels are reversed with high N-Cadherin and low E-cadherin (known as the “cadherin switch” (Maeda et al., 2005). CD10 knockdown in SW480 resulted in a cadherin switch resulting in reduced E-Cadherin expression and increased N-Cadherin expression (Fig. 1, Supplementary Fig. A1) thus complementing the observed changes in cell motility. Evaluation of other EMT markers showed that, despite the cadherin switch and increased motility, Snail and Twist were reduced and Vimentin remained unchanged. However, these changes were not seen with CD10 knockdown in SW620 – there was no cadherin switch and the expression of Snail, Twist and vimentin was unchanged. CD10 Knockdown was associated with slight increase on N-Cadherin and E-Cadherin expression (Fig. 1). Densitometry plots are shown on Supplementary Fig. A1.

3.5. CD10 expression in primary colorectal tumours

Immunohistochemistry for expression of CD10 was performed on a TMA containing 84 primary colorectal cancers. Expression was seen both within the tumour epithelium and the stroma. Within the epithelium there was a mixture of membranous and cytoplasmic expression with varying levels of expression seen. The stromal cells generally showed weaker expression than the epithelium and mostly within the cytoplasm. Representative areas of high or low epithelial and stromal ratio of CD10 immunohistochemical staining are shown on Fig. 5.

Since both stromal and epithelial areas show staining for CD10, automated image analysis software was used to segment out and quantify the level of expression in each compartment. In addition, since cores were taken from 4 different regions (luminal area, mid-tumour, advancing edge and adjacent normal area), each region was examined individually. For an overall evaluation of expression, a total epithelial and stromal score was calculated from the sum of the ratios at the luminal, mid-tumour and advancing edge. To obtain a grade (low or high) of CD10 expression, the epithelial and stromal scores were split in two categories by the median value.

Statistically significant associations were detected between high epithelial CD10 expression and presence of lymph node metastasis (P = .001) and advanced Duke's stage (P = .001). A high stromal CD10 expression was also associated with KRAS wild-type status (P = .043) (Table 2).

Non-parametric Mann-Whitney ranks comparison of the four Duke's stage groups analysed demonstrates statistically significant differences in epithelial CD10 expression are located between Duke's stage A and C1 (P = 0.012) and between stage B and C1 (P = 0.029) (Fig. 6).

4. Discussion

In this study we have examined the role of tumour-associated CD10 in the CRC biology by comparing proliferation, migration and invasion of an isogenic pair of colorectal cancer cell lines derived from different tumour sites (*i.e.* SW480 was derived from the primary tumour whilst SW620 was derived from a metastatic deposit of the same tumour).

CD10 knockdown was achieved by stable lentiviral transduction with PLKO.1-shCD10, confirmed by western blot (Fig. 1). Following stable CD10 knockdown, a reduction in cell viability in SW620^{CD10-} was observed albeit only after 72 h in culture (Fig. 2B). However, in SW480^{CD10-}, there was no significant difference in cell viability (Fig. 2A). Our results can be compared to those obtained by Mizerska-Kowalska et al., who have also observed a reduced proliferation (determined by the BrdU method) and increased proportion of apoptotic cells following CD10 knockdown in the CRC cell line LS180 (Mizerska-Kowalska et al., 2016). In their case however, cell cycle analysis showed G2/M arrest upon transient CD10 knockdown in LS180 cells but not in SW620 (Mizerska-Kowalska et al., 2016). In contrast, although we have observed the same net effect on proliferation following CD10 knockdown, we have obtained a small but significant decrease in G2/M. These small shifts in proliferation could be due to a reduction of focal adhesion kinase phosphorylation at Tyr 397, regulated by CD10 intrinsic signaling (Mizerska-Kowalska et al., 2016). In terms of cell viability and proliferation, we must recognize the nature of the effects of the tumour microenvironment at the primary tumour (SW480) and metastatic site (SW620) and its long term implications in the metabolic activity of the cell lines hereby studied.

Considering the proteolytic function of CD10 and previous associations with cancer progression and metastasis, we had expected that,

in line with published studies (Fujimoto et al., 2005; Fujita et al., 2010; Iwase et al., 2005; Jang et al., 2013; Kuniyasu et al., 2010; Ohji et al., 2007), CD10 silencing would cause a reduction in migration and invasiveness of colorectal cancer cell lines. However our data showed that CD10 silencing resulted in increased migration and invasion of $SW480^{CD10-}$ cell lines, while in $SW620^{CD10-}$ there was no significant change (Fig. 4). Comparable results were obtained by Mizerska-Kowalska et al. who showed that CD10 silencing caused an increase in invasion and migration in LS180. In SW620, they found that CD10 silencing caused increased migration but reduced invasion (Mizerska-Kowalska et al., 2016). This also suggests that CD10 can inhibit cell migration and was attributed to the observation that CD10 silencing induced FAK phosphorylation thereby enhancing cell motility (Mizerska-Kowalska et al., 2016). The reason for the differences in the results in SW620 between our study and that of Mizerska-Kowalska is uncertain but, taking all the data together, there is evidence to suggest that, CD10 can inhibit cell migration.

Knockdown of CD10 in SW480 caused a cadherin shift marked by a decrease in E-cadherin, coupled with an increase in N-cadherin expression (Fig. 1). These results complement our observed differences for migration and invasion. Reduction of E-cadherin, often the result of EMT, is a frequent event during tumour progression and metastasis (Polyak and Weinberg, 2009). Reduced E-cadherin is often accompanied by an increase in N-cadherin during a “cadherin switch” which results in increased cell motility (Maeda et al., 2005). Unexpectedly, the cadherin switch occurred simultaneously with downregulation of Vimentin, Snail and Twist - markers characteristically associated with EMT. This downregulation would usually be associated with reduced motility. The data are suggestive of the plasticity of the mechanisms involved in processes of cell motility and EMT (Grigore et al., 2016; Huang et al., 2013). Loss of E-cadherin expression, with maintenance of high N-cadherin levels is likely to alter the adhesiveness of cells (Chu et al., 2006), and thus may explain the induction of motility without acquisition of a complete EMT shift in $SW480^{CD10-}$. The precise mechanism by which CD10 could be involved in regulating the EMT process by E-cadherin and N-cadherin deserves further investigation.

Published data are inconsistent when IHC for CD10 is evaluated. Some studies have shown high CD10 expression in well and moderately-differentiated colon carcinomas relative to poorly differentiated ones (Fujimoto et al., 2005; Sato et al., 1996). Others have found a progressive increase in CD10 expression from normal to benign tumours to invasive disease (Jang et al., 2013; Yao et al., 2002). In our case only malignant colorectal adenocarcinomas were analysed, and therefore a stepwise association with CD10 expression in normal, benign and malignant tumours could not be made.

While most studies on CD10 have used a positive/negative categorical or semi-quantitative evaluation, we have employed an automated IHC quantification method that excludes the observer-associated subjectivity. When expression of CD10 in the epithelial and stromal tumour compartments was analysed for its associations with clinicopathological variables, high CD10 expression in tumour epithelial cells was associate with advance disease (Dukes' A & B *versus* Dukes' C1 and C2, $P = 0.001$). Differences in CD10 expression were particularly evident in a pairwise ranks comparison between Duke's stage A and C1 ($P = 0.012$) and B and C1 ($P = 0.029$). Stromal CD10 expression was not associated to Duke's stage. Similarly, epithelial CD10 expression was associated with presence of lymph node metastasis ($P < 0.001$). While this is not completely in agreement with our *in vitro* results showing CD10 as an inhibitor of migration and invasion in SW480, *in vivo* epithelial CD10 expression could be counteracting anti-tumoural effect of peptides such as met-enkephalin, and as a consequence, promoting invasion and lymph node metastasis (Kuniyasu et al., 2010). It has also been shown that CD10 enzymatic activity degrades migration-inducing peptides such as bombesin and endothelin (Terauchi et al., 2005; Wang et al., 2017; Zheng et al., 2006). It is therefore feasible that CD10 activitiy *in vivo* is conditioned by the relative abundance of such peptides in different tumour compartments and tumour stages, explaining discrepancies to data obtained *in vitro* where extrinsic peptidase activity of CD10 could not be assessed.

5. Conclusion

Considering the results hereby presented, it is possible that proteolytic effects of CD10-expression are controlled by the surrounding microenvironment and its significance depends on the tumour stage and interaction of stroma and epithelium. Our findings suggest that CD10 knockdown has the potential to increase the migrating and invading ability of the primary colorectal cancer cell line SW480, but not that of the matched metastasis SW620. Intriguingly, results of our TMA analysis on CD10 immunostaining show and association with advanced Duke's stage and presence of lymph node metastasis.

In vitro studies which do not fully recapitulate the rich microenvironment displayed within colorectal tumour could nevertheless suggest alterations in proliferation, migration and invasion together with shifts in EMT markers caused by CD10 knockdown, all of which seem to be influenced by the stage of tumour development. Due to the importance of understanding mechanisms underlying tumour invasion and metastasis, further research is warranted to clarify the role of CD10 in EMT and tumour progression.

Supplementary data to this article can be found online at https://doi.org/10.1016/j.yexmp.2018.04.002.

Acknowledgements

The authors acknowledge financial support from the EC Marie Curie Actions, AIDPATH project (Contract No.612471). Support was also provided by an International Collaborator Award from the Pathological Society of Great Britain and Ireland. Takashi Yao received financial support from Grant-in-Aid for General Scientific Research from the Ministry of Education, Science, Sports and Culture (#17K08704), Japan.

Conflict of interest

Takashi Yao received honoraria for lectures from Takeda Pharmaceutical Co. All other authors declare no conflict of interest.

References

Albasri, A., Fadhil, W., Scholefield, J.H., Durrant, L.G., Ilyas, M., 2014. Nuclear expression of phosphorylated focal adhesion kinase is associated with poor prognosis in human colorectal cancer. Anticancer Res. 34, 3969–3974.

Chu, Y.-S., Eder, O., Thomas, W.A., Simcha, I., Pincet, F., Ben-Ze'ev, A., Perez, E., Thiery, J.P., Dufour, S., 2006. Prototypical type I E-cadherin and type II Cadherin-7 mediate very distinct adhesiveness through their extracellular domains. J. Biol. Chem. 281, 2901–2910. http://dx.doi.org/10.1074/jbc.M506185200.

Fleischmann, A., Schlomm, T., Huland, H., Kollermann, J., Simon, P., Mirlacher, M., Salomon, G., Chun, F.H.K., Steuber, T., Simon, R., Sauter, G., Graefen, M., Erbersdobler, A., 2008. Distinct subcellular expression patterns of neutral endopeptidase (CD10) in prostate Cancer predict diverging clinical courses in surgically treated patients. Clin. Cancer Res. 14, 7838–7842. http://dx.doi.org/10.1158/1078-0432.CCR-08-1432.

Fujimoto, Y., Nakanishi, Y., Sekine, S., Yoshimura, K., Akasu, T., Moriya, Y., Shimoda, T., 2005. CD10 expression in colorectal carcinoma correlates with liver metastasis. Dis. *Colon rectum* 48, 1883–1889. http://dx.doi.org/10.1007/s10350-005-0141-6.

Fujita, S., Taniguchi, H., Yao, T., Shimoda, T., Ueno, H., Hirai, T., Ohue, M., 2010. Multi-institutional study of risk factors of liver metastasis from colorectal cancer: correlation with CD10 expression. Int. J. Color. Dis. 25 (6), 681. http://dx.doi.org/10.1007/s00384-010-0913-x.

Grigore, A., Jolly, M., Jia, D., Farach-Carson, M., Levine, H., 2016. Tumor budding: the name is EMT. Partial EMT. J. Clin. Med. 5, 51. http://dx.doi.org/10.3390/jcm5050051.

Huang, R.Y.-J., Wong, M.K., Tan, T.Z., Kuay, K.T., Ng, A.H.C., Chung, V.Y., Chu, Y.-S., Matsumura, N., Lai, H.-C., Lee, Y.F., Sim, W.-J., Chai, C., Pietschmann, E., Mori, S., Low, J.J.H., Choolani, M., Thiery, J.P., 2013. An EMT spectrum defines an anoikis-resistant and spheroidogenic intermediate mesenchymal state that is sensitive to e-cadherin restoration by a src-kinase inhibitor, saracatinib (AZD0530). Cell Death Dis. 4, e915. http://dx.doi.org/10.1038/cddis.2013.442.

Ibrahim, W.S., 2011. Comparison of stromal CD10 expression in benign, borderline, and malignant phyllodes tumors among Egyptian female patients. Indian J. Pathol. Microbiol. 54, 741–744. http://dx.doi.org/10.4103/0377-4929.91511.

Iwase, T., Kushima, R., Mukaisho, K., Mitsufuji, S., Okanoue, T., Hattori, T., 2005. Overexpression of CD10 and reduced MUC2 expression correlate with the development and progression of colorectal neoplasms. Pathol. - Res. Pract. 201, 83–91. http://dx.doi.org/10.1016/j.prp.2004.09.016.

Iwase, A., Kotani, T., Goto, M., Kobayashi, H., Takikawa, S., Nakahara, T., Nakamura, T., Kondo, M., Bayasula, Nagatomo, Y., Kikkawa, F., 2014. Possible involvement of CD10 in the development of endometriosis due to its inhibitory effects on CD44-dependent cell adhesion. Reprod. Science 21, 82–88. http://dx.doi.org/10.1177/1933719113488449.

Jana, S., Jha, B., Patel, C., Jana, D., Agarwal, A., 2014. CD10-a new prognostic stromal marker in breast carcinoma, its utility, limitations and role in breast cancer pathogenesis. Indian J. Pathol. Microbiol. 57, 530. http://dx.doi.org/10.4103/0377-4929.142639.

Jang, T.J., Park, J.B., Lee, J.I., 2013. The expression of CD10 and CD15 is progressively increased during colorectal Cancer development. Korean J. Pathol. 47, 340–347. http://dx.doi.org/10.4132/KoreanJPathol.2013.47.4.340.

Jiang, W., Hua, R., Wei, M., Li, C., Qiu, Z., Yang, X., Zhang, C., 2015. An optimized method for high-titer lentivirus preparations without ultracentrifugation. Sci. Rep. 5, 13875. http://dx.doi.org/10.1038/srep13875.

Katano, T., Mizoshita, T., Tsukamoto, H., Nishie, H., Inagaki, Y., Hayashi, N., Nomura, S., Ozeki, K., Okamoto, Y., Shimura, T., Mori, Y., Kubota, E., Tanida, S., Kataoka, H., Kuno, T., Takahashi, S., Joh, T., 2017. Ectopic gastric and intestinal phenotypes, neuroendocrine cell differentiation, and SOX2 expression correlated with early tumor progression in colorectal laterally spreading tumors. Clin. Colorectal Cancer 16, 141–146. http://dx.doi.org/10.1016/j.clcc.2016.09.009.

Kuniyasu, H., Luo, Y., Fujii, K., Sasahira, T., Moriwaka, Y., Tatsumoto, N., Sasaki, T., Yamashita, Y., Ohmori, H., 2010. CD10 enhances metastasis of colorectal cancer by abrogating the anti-tumoural effect of methionine-enkephalin in the liver. Gut 59, 348–356. http://dx.doi.org/10.1136/gut.2009.178376.

Lamouille, S., Xu, J., Derynck, R., 2014. Molecular mechanisms of epithelial-mesenchymal transition. Nat. Rev. Mol. Cell Biol. 15, 178–196. http://dx.doi.org/10.1038/nrm3758.

Lloyd, J.M., Owens, S.R., 2011. CD10 immunohistochemistry stains enteric mucosa, but negative staining is unreliable in the setting of active enteritis. Mod. Pathol. 24, 1627–1632. http://dx.doi.org/10.1038/modpathol.2011.122.

Lu, T.-X., Miao, Y., Wu, J.-Z., Gong, Q.-X., Liang, J.-H., Wang, Z., Wang, L., Fan, L., Hua, D., Chen, Y.-Y., Xu, W., Zhang, Z.-H., Li, J.-Y., 2016. The distinct clinical features and prognosis of the CD10 + MUM1 + and CD10 − Bcl6 − MUM1 − diffuse large B-cell lymphoma. Sci. Rep. 6, 20465. http://dx.doi.org/10.1038/srep20465.

Maeda, M., Johnson, K.R., Wheelock, M.J., 2005. Cadherin switching: essential for behavioral but not morphological changes during an epithelium-to-mesenchyme transition. J. Cell Sci. 118, 873–887. http://dx.doi.org/10.1242/jcs.01634.

Maguer-Satta, V., Besançon, R., Bachelard-Cascales, E., 2011. Concise review: neutral endopeptidase (CD10): a multifaceted environment actor in stem cells, physiological mechanisms, and Cancer. Stem Cells 29, 389–396. http://dx.doi.org/10.1002/stem.592.

Mizerska-Kowalska, M., Bojarska-Junak, A., Jakubowicz-Gil, J., Kandefer-Szerszeń, M., 2016. Neutral endopeptidase (NEP) is differentially involved in biological activities and cell signaling of colon cancer cell lines derived from various stages of tumor development. Tumor Biol. 37, 13355–13368. http://dx.doi.org/10.1007/s13277-016-5248-y.

Moffat, J., Grueneberg, D.A., Yang, X., Kim, S.Y., Kloepfer, A.M., Hinkle, G., Piqani, B., Eisenhaure, T.M., Luo, B., Grenier, J.K., Carpenter, A.E., Foo, S.Y., Stewart, S.A., Stockwell, B.R., Hacohen, N., Hahn, W.C., Lander, E.S., Sabatini, D.M., Root, D.E., 2006. A lentiviral RNAi library for human and mouse genes applied to an arrayed viral high-content screen. Cell 124, 1283–1298. http://dx.doi.org/10.1016/j.cell.2006.01.040.

Ogawa, H., Iwaya, K., Izumi, M., Kuroda, M., Serizawa, H., Koyanagi, Y., Mukai, K., 2002. Expression of CD10 by stromal cells during colorectal tumor development. Hum. Pathol. 33, 806–811.

Ohji, Y., Yao, T., Eguchi, T., Yamada, T., Hirahashi, M., Iida, M., Tsuneyoshi, M., 2007. Evaluation of risk of liver metastasis in colorectal adenocarcinoma based on the combination of risk factors including CD10 expression: multivariate analysis of clinicopathological and immunohistochemical factors. Oncol. Rep. 17, 525–530.

Pei, Y., Tuschl, T., 2006. On the art of identifying effective and specific siRNAs. Nat. Methods 3, 670–676. http://dx.doi.org/10.1038/nmeth911.

Polyak, K., Weinberg, R.A., 2009. Transitions between epithelial and mesenchymal states: acquisition of malignant and stem cell traits. Nat. Rev. Cancer 9, 265–273. http://dx.doi.org/10.1038/nrc2620.

Puri, V., Jain, M., Mahajan, G., Pujani, M., 2016. Critical appraisal of stromal CD10 staining in fibroepithelial lesions of breast with a special emphasis on expression patterns and correlation with WHO grading. J. Cancer Res. Ther. 12, 667–670. http://dx.doi.org/10.4103/0973-1482.177215.

Sasaki, T., Kuniyasu, H., Luo, Y., Fujiwara, R., Kitayoshi, M., Tanabe, E., Kato, D., Shinya, S., Fujii, K., Ohmori, H., Yamashita, Y., 2014. Serum CD10 is associated with liver metastasis in colorectal cancer. J. Surg. Res. 192, 390–394. http://dx.doi.org/10.1016/j.jss.2014.05.071.

Sato, Y., Itoh, F., Hinoda, Y., Ohe, Y., Nakagawa, N., Ueda, R., Yachi, A., Imai, K., 1996. Expression of CD10/neutral endopeptidase in normal and malignant tissues of the human stomach and colon. J. Gastroenterol. 31, 12–17. http://dx.doi.org/10.1007/BF01211181.

Tariq, M.U., Haroon, S., Kayani, N., 2015. Role of CD10 Immunohistochemical expression in predicting aggressive behavior of Phylloides tumors. Asian Pac. J. Cancer Prev. 16, 3147–3152.

Terauchi, M., Kajiyama, H., Shibata, K., Ino, K., Mizutani, S., Kikkawa, F., 2005. Anti-progressive effect of neutral endopeptidase 24.11 (NEP/CD10) on cervical carcinoma in vitro and in vivo. Oncology 69, 52–62. http://dx.doi.org/10.1159/000087476.

Wang, Z., Liu, P., Zhou, X., Wang, T., Feng, X., Sun, Y.-P., Xiong, Y., Yuan, H.-X., Guan, K.-L., 2017. Endothelin promotes colorectal tumorigenesis by activating YAP/TAZ. Cancer Res. 77, 2413–2423. http://dx.doi.org/10.1158/0008-5472.CAN-16-3229.

Yao, T., Takata, M., Tustsumi, S., Nishiyama, K., Taguchi, K., Nagai, E., Tsuneyoshi, M., 2002. Phenotypic expression of gastrointestinal differentiation markers in colorectal adenocarcinomas with liver metastasis. Pathology 34, 556–560.

Zheng, R., Iwase, A., Shen, R., Goodman, O.B., Sugimoto, N., Takuwa, Y., Lerner, D.J., Nanus, D.M., 2006. Neuropeptide-stimulated cell migration in prostate cancer cells is mediated by RhoA kinase signaling and inhibited by neutral endopeptidase. Oncogene 25, 5942–5952. http://dx.doi.org/10.1038/sj.onc.1209586.